ELSEVIER

Acta Psychologica 107 (2001) 229–247

acta psychologica

www.elsevier.com/locate/actpsy

Abnormal retinotopic representations in human visual cortex revealed by fMRI

Antony B. Morland [a,*], Heidi A. Baseler [c], Michael B. Hoffmann [a], Lindsay T. Sharpe [b], Brian A. Wandell [c]

[a] *Psychology Department, University of London, Royal Holloway, Egham, Surrey TW20 0EX, UK*
[b] *Psychology Department, Newcastle University, Newcastle, UK*
[c] *Psychology Department, Stanford University, CA 93155, USA*

Received 1 September 2000; received in revised form 8 December 2000; accepted 11 December 2000

Abstract

The representation of the visual field in early visual areas is retinotopic. The point-to-point relationship on the retina is therefore maintained on the convoluted cortical surface. Functional magnetic resonance imaging (fMRI) has been able to demonstrate the retinotopic representation of the visual field in occipital cortex of normal subjects. Furthermore, visual areas that are retinotopic can be identified on computationally flattened cortical maps on the basis of positions of the vertical and horizontal meridians. Here, we investigate abnormal retinotopic representations in human visual cortex with fMRI. We present three case studies in which patients with visual disorders are investigated. We have tested a subject who only possesses operating rod photoreceptors. We find in this case that the cortex undergoes a remapping whereby regions that would normally represent central field locations now map more peripheral positions in the visual field. In a human albino we also find abnormal visual cortical activity. Monocular stimulation of each hemifield resulted in activations in the hemisphere contralateral to the stimulated eye. This is consistent with abnormal decussation at the optic chiasm in albinism. Finally, we report a case where a lesion to white matter has resulted in a lack of measurable activity in occipital cortex. The activity was absent for a small region of the visual field, which was found to correspond to the subject's field defect. The cases selected have been chosen to demonstrate the power of fMRI in identifying abnormalities in the cortical representations of the visual field in patients with visual dysfunction. Furthermore, the experiments are able to show how the cortex is capable of modifying the visual field representation in response to abnormal input.

* Corresponding author.

0001-6918/01/$ - see front matter
PII: S0001-6918(01)00025-7

PsycINFO classification: 2323; 2520; 2820

Keywords: Visual area; Photoreceptor; Lesion; Functional imaging; Patients; Albino; Rod achromat

1. Introduction

In primates, the cortical representation of the visual field in early visual areas is retinotopic. That is, neighbouring points on the retina project to neighbouring points on the cortical surface. In this article we focus on abnormal retinotopic cortical maps in human. We have studied patients with different visual dysfunction, which arise at different sites on the visual pathway. We endeavour to reveal the potential for the cortex to reorganise in the light of abnormal retinal input, and how visual cortical signals can reveal the underlying cause of visual field defects. For each of the studies described we concentrate on the cortical representation of the visual field that can be documented with functional magnetic resonance imaging (fMRI). We review briefly the evidence for retinotopic representations of the visual field in the human visual cortex. This is followed by a description of the general methods used to map retinotopic areas of the human occipital lobe with fMRI. Three case studies that demonstrate abnormal retinotopic representations in human visual cortex are then presented.

Holmes (1918) was able to determine the topographic mapping of the visual field onto calcarine cortex by documenting visual field defects of soldiers who suffered gunshot wounds to the occipital lobe. More detailed lesion studies along similar lines have allowed a fuller picture of the topographic cortical representation to be gained (Horton & Hoyt, 1991a; Sharpe & Wong, 1997). Studies of human patients with damage to extrastriate regions of the visual cortex revealed the nature and extent to which visual processing depended on areas beyond the calcarine sulcus (Clarke, Walsh, Schoppig, Assal, & Cowey, 1998; Damasio, Yamada, Damasio, Corbett, & McKee, 1980; Kennard, Lawden, Morland, & Ruddock, 1995; Zihl, von Cramon, & Mai, 1983). In addition, extrastriate lesions were shown to result in visual deficits that are restricted to one quadrant of the visual field (Horton & Hoyt, 1991b). This finding indicated that extrastriate visual areas in dorsal and ventral cortex represent the lower and upper quadrants of the visual field, respectively. Although a considerable amount is known about the visual representation in the human occipital lobe from lesion studies, electrophysiological primate studies have been able to reveal greater detail of the cortical representations of the visual field (Hubel & Wiesel, 1974; Tootell, Switkes, Silverman, & Hamilton, 1988).

Over the last decade functional imaging methods have emerged, which have allowed visual areas of the human brain to be identified and their properties measured (Engel, Glover, & Wandell, 1997; Sereno et al., 1995; Tootell, Dale, Sereno, & Malach, 1996; Zeki et al., 1991). These developments have profound implications on the study of patients with visual dysfunction. The patient can now undergo func-

tional imaging so that information concerning the impact of the lesion on cortical activity elsewhere can be gained (Barbur, Watson, Frackowiak, & Zeki, 1993; Barton et al., 1996; Baseler, Morland, & Wandell, 1999; Sahraie, Weiskrantz, Simmons, Williams, & Barbur, 1996; Zeki & Ffytche, 1998). This represents a great advance, as human lesions are seldom loyal to any boundary that may divide different visual areas, so interpretation on the basis of anatomy alone is error prone. Lesions often involve white matter, and the consequences of such damage on intact cortical structures can only be assessed by measurement and localization of cortical activity. Furthermore, the effects on cortical visual representations of abnormalities that occur at earlier stages of the visual system can also be documented with functional imaging.

Perhaps the most successful implementation of functional imaging in assessing visual cortical function is the retinotopic mapping method based on fMRI. An early study revealed how visual field eccentricity was mapped along the calcarine sulcus (Engel et al., 1994). Studies by the same group (Engel et al., 1997) and others (DeYoe et al., 1996; Sereno et al., 1995) described methods by which visual areas could be identified on the basis of the cortical representations of vertical and horizontal meridians of the visual field. The same criterion for identifying different retinotopic maps had also been established in the studies that evaluated the cortical patterns of neural degeneration associated with sectioning the corpus colosum in monkey (Zeki, 1977) and human (Clarke & Miklossy, 1990).

In this article we will review three different studies that investigate the impact of visual dysfunction on cortical visual responses. The studies differ in the sense that the subjects have visual deficits that are expressed at different levels of the visual system. We first describe the effects on the cortical visual maps of abnormal retinal receptor distributions that are found in rod monochromacy. This study documents how the cortex is able to reorganize in response to abnormal input signals. On a similar theme, we examine how the cortical signals are arranged in human albinos. In human albinism the principal deficit occurs at the optic chiasm, where fibres undergo almost complete crossing unlike the normal pattern in which approximately half of the fibres project contralateral to the eye. We then describe how visual field defects can be documented with retinotopic mapping techniques in the case of cortical lesion. The theme is to demonstrate how the application of fMRI to cases of abnormal vision can reveal properties of the human visual system that are not highlighted by the study of normal vision.

2. Methods

In conventional functional magnetic imaging experiments a difference between the blood oxygenation level dependent (BOLD) signal is measured in response to a difference between two different stimulus or task conditions. Reversing checkerboard patterns with uniform grey control periods were presented cyclically during fMRI in some of the first experiments used to evaluate the potential of fMRI to measure cortical activity. In order to determine the nature of the visual field

representation in human cortex, however, a modification of this general scheme was developed. The technique relies on the same general principal that visual stimulation is contrasted with a control condition. The key step, however, was to stimulate different field locations at different times (DeYoe, Bandettini, Neitz, Miller, & Winans, 1994; Engel et al., 1994; Sereno et al., 1995). With such a scheme position in the visual field is encoded in the time domain. The onset of the neural response thus encodes the visual field position to which the region of cortex is responsive. Due to hemodynamic delays the BOLD signal evolves slowly compared to the neural response. A correction to the time of onset of the BOLD response has to be made, therefore, in order to establish correctly the cortical representation of the visual field.

Although it would be possible to stimulate different field locations at different times in a random fashion, researchers used stimuli that moved progressively through regions of the visual field. Two principal variants of these stimuli exist, those that moved progressively through increasing eccentricity and those that rotated around the point of fixation thereby stimulating consecutively polar angle. Stimuli that step through eccentricity usually comprise a series of ring elements (see inset in Fig. 1). A subset of neighbouring rings undergoes pattern reversal at any one time, after which one element is extinguished and another commences pattern reversal. The net effect is a stepwise movement of a ring through increasing eccentricity. Consequently cortex representing central visual field locations will respond at an earlier phase in the cycle than cortex representing more peripheral locations. As a result an eccentricity map is obtained. Similarly, a map of the representation of the polar angle of the visual field is obtained with the visual stimulus that rotates around fixation comprises a wedge with its apex centred on fixation. These experiments yield the cortical locations of the horizontal and vertical meridians. Visual areas are delimited by the meridian representations. Different research groups have used wedges of different fractions of a full circle; in the studies we describe here a quadrant of the full circle is used (Fig. 3(a)). As with the ring stimuli the checkerboard wedge undergoes pattern reversal and then assumes the next position and so on to describe a full rotation. For both stimulus regimes appropriate stimulus duration and delay between stimulation at different field locations are selected in order to account for the speed at which the cortical activity could be measured with fMRI (Boynton, Engel, Glover, & Heeger, 1996). In the experiments we describe here, one full cycle of the stimulus lasts 36 s, which is well within the temporal resolution of the BOLD signal.

The methods described above allow the cortical representation of the visual field to be determined. However, the representation is expressed in the 2-D cross sectional slices of the brain acquired with fMRI. The crucial step required to identify visual areas and evaluate cortical representations of the visual field is to project functional data onto a flattened representation of the cortical grey matter. This allows the visual field representation to be visualized on the cortical surface. This fundamental aspect of the method was developed in parallel by a number of groups (Dale, Fischl, & Sereno, 1999; Drury et al., 1996; Fischl, Sereno, & Dale, 1999; Teo, Sapiro, & Wandell, 1997). The computational methods used by all groups are based on

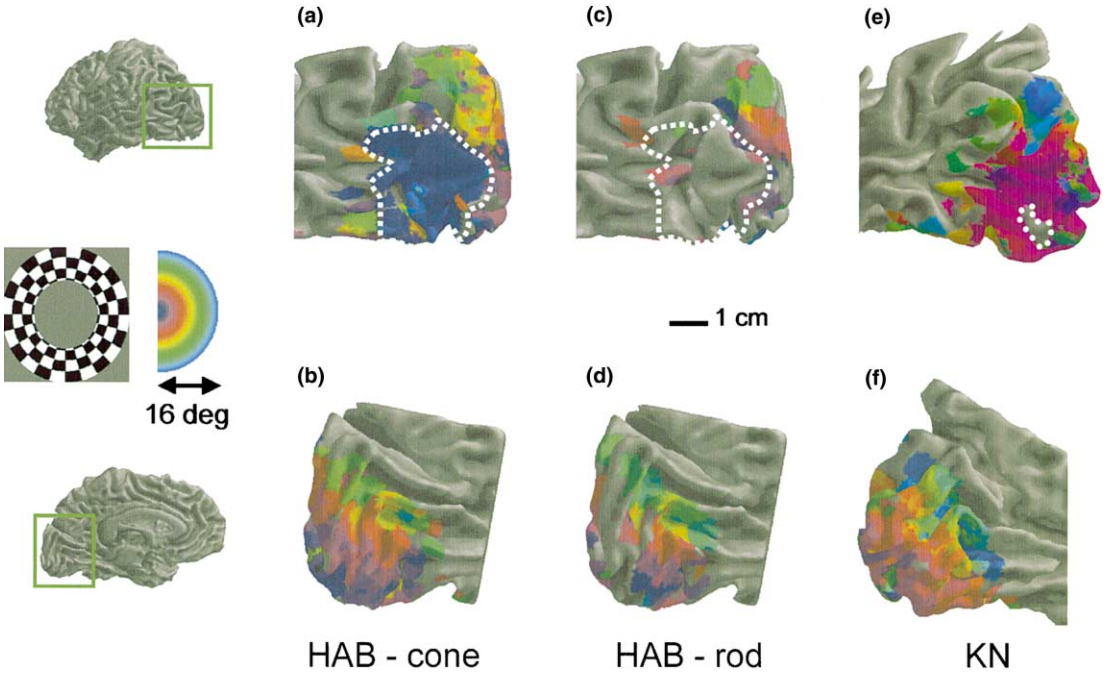

Fig. 1. Cortical representations of eccentricity for subjects HAB ((a)–(d)) and KN ((e) and (f)). To the left of the figure are views of the cerebral hemispheres of the subjects that indicate the region of cortex that is displayed at greater magnification in the panels (a)–(f). Also illustrated is a schematic of the visual stimulus and a colour key for the mapping of eccentricity. (a) and (b) indicate the cortical mapping of eccentricity for a stimulus that isolated the L-cones only in the normal subject HAB. Central regions of the visual field occupy a large lateral region of cortex. A broken line has been drawn to indicate the area of cortex, which is activated by stimuli falling in the central 2° of visual field. In panels (c) and (d) the activity is plotted for a stimulus that was viewed by HAB at low light levels in order to stimulate rods only. In this case the region that is normally driven by central visual field appears to have no significant activations. The broken line drawn in (a) has been added to figure (c) to indicate the area of cortex normally responsive to the central 2°. Cortical activitations measured in KN are shown in panels (e) and (f). In (e), it is clear that significant activations are observed through the majority of the medial aspect of the occipital lobe unlike those in the control (c). The broken line in (e) indicates the small region within which activations were not significant in KN.

maintaining point-to-point relationships in the convoluted surface of grey matter in a two-dimensional (2-D) map. This is physically impossible to do without cutting the 3-D surface. Given the complexity of the cortical surface it is impractical to introduce the number of cuts that would be required to generate a perfect solution to the computational problem, so although some groups have introduced cuts all methods remain approximations. The residual distortions in the flattening procedures are of the order of 15% (Drury et al., 1996; Sereno et al., 1995).

The retinotopic mapping technique takes advantage of the strengths of MRI. Functional information can be measured with spatial precision of the order of 1mm. This is vital if the responses to different positions in the visual field are to be resolved. It is noteworthy that no other imaging technique has been able to resolve the visual maps of the human cortex on the basis of retinotopy. The flattened representation of grey matter again relies on the unparalleled spatial resolution achieved in conventional T1 weighted anatomical MRI and the contrast in the grey and white matter signals that allows the segmentation of these tissue types. In the case studies reported below, two different scanners were used and details of the scanning procedures are given for each investigation.

3. Results

3.1. Cortical topography in rod achromats

Rod achromats have been shown to have a specific genetic abnormality that affects the phototransduction in the cone photoreceptors (Kohl et al., 2000; Kohl et al., 1998). That is, the cone cells are thought to be normal, but the process that normally occurs within them is absent. The rod photoreceptors, however, remain unaffected. Rod achromats have visual function that closely resembles that of a normal under very low (scotopic) light levels (e.g., Hess, Mullen, Sharpe, & Zrenner, 1989; Sharpe, Fach, & Nordby, 1988). Rod achromats have poor visual acuity, principally because of the lack of functioning photoreceptors in the fovea where cones are tightly packed to sample the retinal image at high resolution. Furthermore, rod achromats are photophobic and need to wear dense spectacles, which usually transmit long wavelengths only, in order to perform activities under everyday lighting conditions. Rod achromats also suffer from nystagmus, which is often more severe under high than low light levels.

Studying these observers gives an ideal opportunity to explore the way in which cortical maps develop when the input provided by foveal cones is absent. In normal subjects the cortex has a disproportionately large foveal representation (e.g., Engel et al., 1997). Given the recent estimates of the human cortical magnification factor (Engel et al., 1997; Sereno et al., 1995) the central 1° of visual field is represented by approximately 520 mm^2 of primary visual cortex. In normal subjects, therefore, rod signals are unlikely to encroach on a 520 mm^2 region of visual cortex. Does the cortex in achromatic subjects exhibit the same pattern of cortical mapping or does reorganization of the visual maps occur in response to abnormal cortical input?

Here we address this question by applying retinotopic mapping procedures to a rod achromat, KN. KN, aged 56, has been studied extensively and exhibits visual function consistent with the complete absence of cone photoreceptors. His fixation was remarkably stable with nystagmus of amplitude generally less than 1° (based on scanning laser ophthalmoscopic measurements). KN also has a central scotoma which has been estimated to be between 10 min and 1°, but estimates are error prone due to nystagmus. The stimulus comprised a checkerboard circle and annuli that were centred on fixation. At any one time half of the elements were displayed contiguously and underwent pattern reversal at 4 Hz. The stimulus started centrally and expanded in a stepwise fashion to an eccentricity of 16°, at which point the stimulus started again centrally. This stimulus cycle lasted 36 s and was repeated seven times. Each field location was stimulated by the pattern reversal for 18 s with the remaining 18 s received a uniform grey stimulus. As described in the Methods section, the phase of the alternation between the pattern reversal and the uniform grey indicates the stimulus location. Correspondingly, a measure of the phase of the cortical response determines the location to which the cortex responds. In order to provide a clear fixation guide we presented throughout the experiment a static cross centred on the expanding pattern of 16° radial extent. The retinotopic mapping stimuli were also modified to stimulate selectively different receptor classes. Rods were selectively stimulated in both KN and the control subject HB by reducing the overall stimulus luminance to 0.08 cd/m^2 at which level cones are unresponsive. We also used a silent substitution method (Estevez & Spekreijse, 1982) to design an L cone isolating stimulus to present to the control subject HB. The stimulus was also presented at a higher (80 cd/m^2) luminance. Magnetic resonance images were acquired using a 1.5 T GE Signa scanner fitted with a special purpose head coil (for anatomical imaging) and surface coil (for functional images). Anatomical images were acquired with a resolution of $0.9 \times 0.9 \times 1.2$ mm^3. Functional images were acquired every 3 s using a two-shot, 2-D spiral gradient-recalled echo sequence [echo time: 40 ms, repetition time: 1500 ms, flip angle: 90°, voxel size: $1 \times 1 \times 4$ mm^3].

The results of the study are presented in Fig. 1 in which the phases of the cortical activations are presented in pseudo-colour on the surface of the cortex. The normal cortical representation of signals originating from cone photoreceptors displays the characteristic distribution with a large posterior and lateral representation of the centre of the visual field, shown in blue (Fig. 1(a) and (b)). In contrast, when the control subject views the stimulus under scotopic conditions (Fig. 1(c) and (d)) there is an absence of highly correlated activations in the same cortical region. The mapping of peripheral visual field, however, appears to be very similar on the medial aspect of the occipital lobe, indicating that rod and cone signals activate common cortical regions for non-foveal visual stimulation (Fig. 1(b) and (d)). The data for the normal allow the region of cortex driven by foveal cones to be identified and the broken line in the figure highlights this region. The data for the rod achromat (Fig. 1(e) and (f)) reveal that visual stimulation activates cortex in a coextensive area that would normally be driven by cone signals in the normal subject. That is, the foveal representation has been recruited by rod driven signals, and little cortex remains silent based on our fMRI measurements. The extent to which the cortex is appropriated by rod signals in this subject is of the order of 200 mm^2.

What is the significance of this result? We believe that the encroachment by rod driven signals of cortical territory usually driven by only cone signals represents a large change in the cortical representation of the visual field that is dependent on visual experience. To reach this conclusion we put forward the following argument. At birth the visual afferents from the retina in a rod achromat are structurally normal, that is, the cones appear normal and the ganglion cells that are cone driven are also in place. At birth, therefore, the number of fibres representing foveal visual field is normal. Furthermore, the anatomical connections from the retina to the thalamus and then cortex are principally laid down before birth. So, it is likely that the wiring scheme that gives rise to the normal representation of the visual field is established at birth. In rod achromats, however, signals within the central fovea are not light driven. We believe that the abnormal signaling from the retina results in a downstream reorganization of the cortical representation of the visual field. It should be noted that the reorganization could not be accounted for by abnormal fixation in this subject. No amount of eye movement can generate light driven signals in a region of retina for which there exist no operative photoreceptors (as documented by KN's scotoma). Our finding that the cortex reorganizes is consistent with that shown in monkey cortex when the retina is lesioned (Heinen & Skavenski, 1991). The extent of the reorganization is, however, greater here (>10 mm) than in animal models (~6 mm).

3.2. The visual cortical representation in human albinism

Albinism is a genetic abnormality that affects the production of the pigment melanin. In oculocutaneous albinism this results in characteristic hypopigmentation of the skin, hair, iris and retinal epithelia. In ocular albinism only the iris and retinal epithelia are affected. In both classes of albinism, however, the absence of melanin affects the development of the visual projection from the retina to the brain. The principal abnormality is the mis-routing of fibres at the optic chiasm, which was first observed in rat (Lund, 1965) and subsequently in cat (Creel, 1971; Guillery, 1969; Hubel & Wiesel, 1971), ferret (Guillery, 1971), monkey (Guillery et al., 1984) and human (Guillery, Okoro, & Witkop, 1975). In the normal human the fibres originating from temporal retina project to cortex ipsilateral to the eye, whereas fibres originating from nasal retina cross at the optic chiasm to project contralaterally. In the albino, however, a large proportion of temporal fibres also crosses at the optic chiasm (Guillery et al., 1975). The line of decussation is, therefore, shifted to temporal retina. The albino LGN is abnormal because neighbouring layers do not contain overlapping representations of the visual hemifield originating from different eyes as they do in normal (Guillery, 1974). The cortex, therefore, is fed information in an abnormal format. This has profound implications on the way in which the visual field is topographically mapped onto the surface of the cortex. In various animal models the cortical arrangement of signals has been documented.

Three clear, but very different, patterns have emerged. These patterns are referred to as the 'Albino', the 'Midwestern' and 'Boston' representations. They can be best explained following a description of the normal projection from the LGN to cortex.

The neighbouring layers in the normal LGN are occupied by representations (in register) of the same hemifield, but originate from different eyes. The information from neighbouring layers then project to the cortex, where neighbouring points represent the same position in the visual field, but originate from different eyes. This pattern is systematic in the input layer of V1 and forms that characteristic pattern of ocular dominance columns. In the Albino pattern, the geniculo-cortical projection maintains the normal wiring (Guillery, 1986), but because the layers of the LGN represent mirror symmetric positions about the vertical meridian, this causes the representation of each hemifield to be superimposed. This can be thought of as the ocular dominance columns now representing equal, but opposite eccentricities. The Midwestern cortical representation described in Siamese cat (Kaas & Guillery, 1973) also results from geniculate afferents targeting the same cortical sites as they would in normal. This pattern is different from the Albino pattern because the cortical representation of the abnormally crossed fibres is weak, and behaviourally cats with the Midwestern pattern fail to respond to light stimuli presented to the nasal field. So, although there is no significant rerouting of fibres, the manner in which the cortex deals with the signals requires some intracortical suppression. Hubel and Wiesel (1971) described an arrangement, later referred to as the Boston pattern, in which the abnormally crossing fibres from temporal retina form a cortical representation contiguous with the normal map. As a whole, therefore, the cortical representation remains retinotopic and covers a larger than normal region of the visual field. Considerable rewiring of the geniculo-cortical projection is required for this cortical pattern to emerge. To summarise, in the Midwestern and Albino pattern the geniculo-cortical wiring does not undergo change and visual field locations that are mirrored about the vertical meridian occupy neighbouring points in cortex. In the Boston pattern significant reorganisation occurs to allow the aberrant retinal input to be represented retinotopically in cortex.

There is little information concerning the human albino visual projection. Visual evoked potentials (VEP) have been used clinically to demonstrate reliably albino misrouting (Apkarian, 1992). VEP signals were found to be predominantly over the hemisphere contralateral to the stimulated eye in albinos. This finding has also been confirmed by one recent fMRI study (Hedera et al., 1994). In the fMRI study the stimuli presented were full field. This stimulus scheme is able to elucidate the abnormal albino pathway, but is not capable of revealing how the different visual hemifields map onto the cortical surface. The aim of the case study we describe here is to evaluate how the information from each hemifield is represented in the human albino visual areas.

In order to address our aim we presented stimuli to the right and left hemifields of an albino viewing monocularly. Two experiments were performed in order to determine the answer to two questions. Firstly, do stimuli presented to each hemifield generate cortical activity? Secondly, if activity is elicited by stimuli presented to each hemifield, do they drive different or the same cortical locations? These two questions are attempts to establish the rules by which the aberrant input to cortex is dealt with by the brain and how, in human, this may relate to previous data obtained from animal models.

We presented a high contrast checkerboard pattern that reversed a 6 Hz and appeared in either the right or left hemifield (see illustration in Fig. 2 for the spatial arrangement of the stimulus). The pattern was positioned such that it was at least 2.5° from a central fixation cross. This feature of the stimulus was implemented in order to be certain that the stimulus remained in the desired hemifield as the patient suffered nystagmus of an amplitude smaller than 3°. The stimulus cycle comprised presentation of the checkerboard for 18 s followed by a uniform grey control period of the same duration and mean luminance level. The stimulus cycle was repeated seven times and eight T2* images perpendicular to the calcarine sulcus were obtained every 3 s for the duration of the experiment (252 s – 84 temporal samples). The functional MR images were acquired using a Siemens Magnetom Vision 1.5 T MRI system fitted with EPI gradient overdrive. A Multi-slice 2D gradient echo EPI sequence (TE 54 ms, 128×128 matrix, 240 mm Field of View, interleaved slice order with no gap) was used to measure the BOLD signal as a function of time. The image planes were 4 mm thick, giving voxel dimensions of $1.82 \times 1.82 \times 4$ mm^3. Anatomical images were obtained using the same scanner using the MPRAGE sequence with a voxel size of $0.98 \times 0.98 \times 1$ mm^3.

We tested a 55 year old, tyrosinase positive, female albino, who had best corrected acuity of 0.33 and nystagmus no greater than 3° in amplitude. The albino subject required refractive correction in order to achieve her best acuity and this was provided by fitting trial lenses to a non-metallic trial frame during scanning. Three control subjects were tested, aged between 26 and 33 and with normal visual acuity. We present here the data for one subject, EA, who displays the characteristics expressed in all the control subjects. Both subjects were tested *monocularly* and viewed the stimuli with their right eye.

The results for hemifield stimulation in the normal and albino are displayed in Fig. 2(a). The data are represented on flattened representations of the occipital lobe and are for voxels that exceed a correlation threshold of 0.25. Voxels have been blurred with a Gaussian kernel (S.D. = 10 mm). In the top row the cortical activations in response to stimulation of the right hemifield are shown for the left and right hemispheres of the normal (left of the figure) and albino (right of the figure). The normal's left hemisphere has three patches of activation one of which is in the fundus of the calcarine sulcus. It is likely that the activations reflect the cortical representations of the horizontal meridian, with the V1 representation in the calcarine cortex and the V2/V3 boundaries superior and inferior to the calcarine sulucus. Activations in the right hemisphere of the normal did not exceed the correlation threshold of 0.25. In the albino, stimulation of the right hemifield also resulted in activation in the calcarine sulcus of the left hemisphere, with effectively no activation observed in the right hemisphere. It should be noted, however, that the pattern of activations in the albino cortex is not as extensive as in normal and although there is activity in what may be assumed to be V1, there is no evidence of activations at the regions that correspond to the V2/V3 boundaries in normal. Both subjects viewed the right hemifield stimulus through the right eye, so the nasal retina was stimulated. Fibres from nasal retina are expected to cross to the hemisphere contralateral to the eye in both normal and albino. The results shown in Fig. 2(a) are entirely consistent,

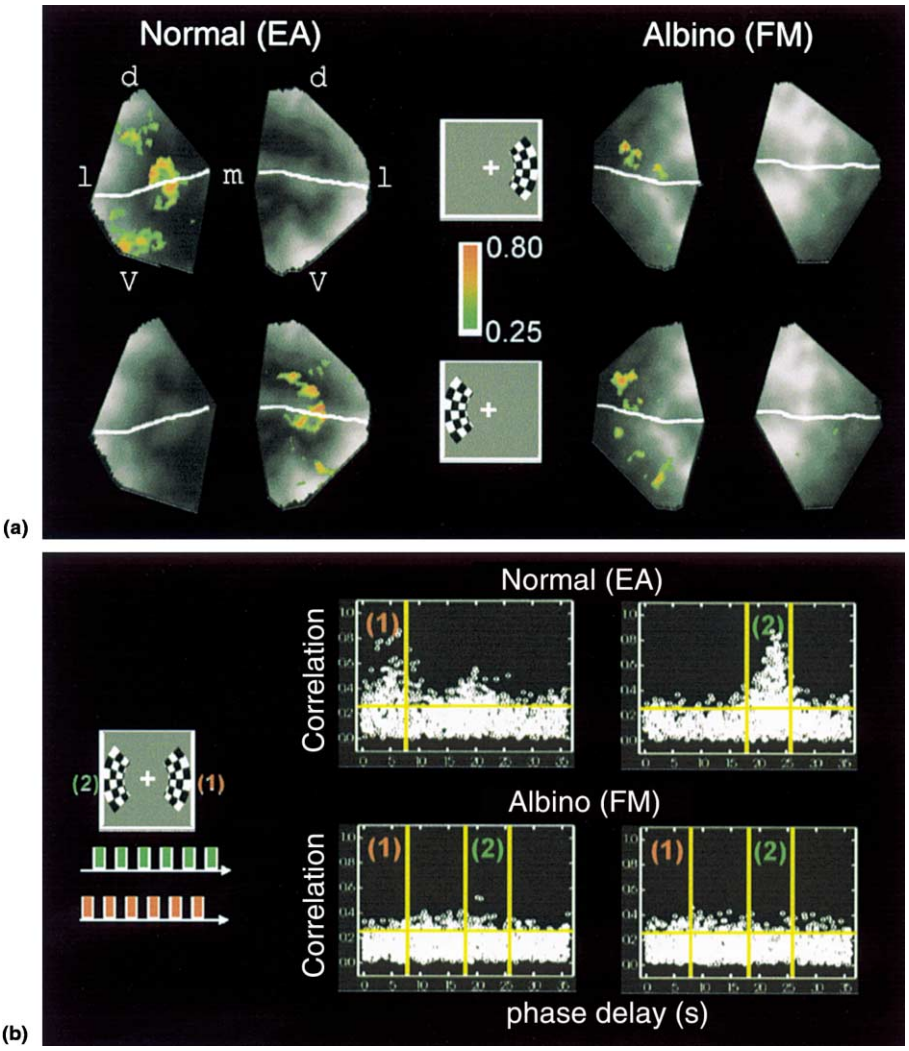

Fig. 2. (a) Flattened representations of the occipital lobes of the left and right hemispheres of subjects EA and FM. In each pair of images the dorsal (*d*), ventral (*v*), lateral (*l*) and medial (*m*) follow the same pattern as shown in the upper left pair of images. In each image the fundus of the calcarine is marked as a solid white line. The colour code bar indicates the correlation coefficient values plotted in the flat maps, which ranged from 0.25–0.80 in EA and from 0.25–0.80 in FM. The upper pairs of images correspond to activations recorded in the normal (EA) and albino (FM) in response to stimulation of the right hemifield (see stimulus inset). In both cases activations exceeding 0.25 correlation are in the left hemisphere only. Pairs of images for stimulation of the left hemifield indicate that the right hemisphere is activated in the normal (EA) but the left is activated in the albino (FM). (b) Plots of the voxel correlation as a function of phase delay for all grey matter voxels in subjects EA and FM. Plots to the left and right are for the grey matter voxels derived from the left and right hemispheres, respectively. The visual stimulus is shown to the left of the plots and below it is the stimulus cycle for the right (1) and left (2) visual field stimulation.

therefore, with the anticipated projection pathways in normal and albino. Furthermore, it can also be seen that the normal's results are consistent with retinotopic representations of the visual field in the occipital lobe.

In the bottom row of Fig. 2(a) data are presented that highlight the difference between the normal and albino visual projection. In this case the stimulus is presented in the left hemifield so that the temporal retina of the right eye is stimulated. For the normal the right hemisphere is activated by the left hemifield stimulus, but no activations exceed 0.25 correlation in the left hemisphere. The pattern of activation is similar to that exhibited in the left hemisphere during right field stimulation, but activation below the calcarine sulcus is less extensive. For the albino, however, the only activations to stimulation of the left hemifield arise in the left hemisphere. The pattern of activations appears different from that elicited by stimulation of the right hemifield. More extensive activation is present superior and inferior to the calcarine sulcus when the left hemifield is stimulated than when stimulation is to the right hemifield. Does this mean that the two hemifields map to different cortical regions? We attempt to address this question further in an experiment that alternates between stimulation of the right and left hemifields.

The stimulus used to probe the cortical representation of the visual field in albism is shown in Fig. 2(b). It comprises both the checkerboard elements of the stimuli used in two previous experiments. In this case, however, the checkerboard elements were presented in temporal antiphase, such that the right hemifield was stimulated for 18 s followed by 18 s of stimulation of the left hemifield. In the normal subject this stimulus design resulted in strong activations of the left hemisphere when the stimulus was presented to the right hemifield, but no significant activations in response to stimulation of the left hemifield. Conversely, in the right cortex activations were only observed at phases consistent with stimulation of the left hemifield. So, the stimulus drove activity in the left and right hemispheres at different times. If the cortical representations of the left and right hemifields are different in the albino, the cortex should respond at different times in a similar manner to that of the normal's. In contrast to the normal, however, the activations would be anticipated to originate from the same cortical hemisphere given the results shown in Fig. 2(a). However, no activations in albino cortex exceed threshold (0.25) in response to sequential stimulation of right and then left hemifields. It would appear, therefore, that at the resolution of fMRI, the representations of the left and right hemifields in early cortical areas occupy the same locations. This result appears to be at odds with the experiments in which the right and left hemifields were stimulated in isolation. The difference could be that the activations shown in Fig. 2(a), although located differently, could have resulted from different fixation positions in the two different experiments.

The results of three experiments allow us to draw two conclusions concerning the albino visual pathway. Firstly, the albino cortex is driven by both hemifields, which has been previously inferred from VEP studies (Apkarian, 1992). Evidence from animal models suggest that the aberrant input to the cortex of Midwestern cats from temporal retina may be suppressed. Our results do not support this finding and suggest that in this human albino the Midwestern pattern is not expressed. The third

experiment does not indicate that the representation of the temporal retinal signals is mapped to a different region of cortex from the nasal retinal signals, which rules out the Boston pattern. It would appear, therefore, that the most likely arrangement to describe our results is the Albino pattern. Further studies on other albino patients may reveal the extent to which this pattern may be conserved amongst human albinos. In the Midwestern Siamese cat colony it is interesting to note that Midwestern patterns were expressed in 90% of cats and Boston in the remaining 10%, and vice versa in the Boston colony (Guillery, 1986). This indicates that the gross reorganization found in the Boston pattern is a likely consequence of developmental and not genetic factors. Similar effects are likely, therefore, in the human population.

3.3. Mapping field defects

As outlined in Section 1, the retinotopic nature of the human cortical representation of the visual field was elucidated by studies of gunshot wound victims, who sustained lesions to the calcarine cortex of occipital lobe (Holmes, 1918). However, there are often cases where lesions located in regions other than calcarine cortex give rise to visual field losses. These cases do not provide the compelling evidence for a retinotopic mapping that the studies of patients with lesions to calcarine grey matter do. Here we present such a case, where a 43 year-old patient (SA) presented with difficulties in reading, but standard perimetry revealed a questionable central scotoma. Retinotopic mapping was subsequently performed with fMRI and an absence of cortical activity was observed for stimulation of a small ($<3°$) lower right quadrant of the visual field. Follow-up perimetry measurements that sampled the visual field with greater spatial resolution also revealed a scotoma in the lower right central region of the visual field. MRI demonstrated a left parieto-occipital mass, which was excised and identified as a metastasis. The surgery resulted in a unilateral lesion to the left occipital lobe. The lesion does not involve calcarine grey matter and other medial aspects of the occipital lobe appear intact. Our imaging experiments were performed 9 months following surgery. On examination her distance visual acuity with spectacles was 6/5 bilaterally and she was able to read N5 (a test of reading near text, where N5 reflects normal vision much as 6/6 acuity would for more distant vision) with each eye. Her colour vision, pupillary responses and eye movements were normal. There were no abnormalities of the anterior chamber, media, retina or discs on slit lamp examination. Her visual fields were full to confrontation with hand movements, but perimetry (Humphrey) demonstrated a homonymous scotoma in the central 3° of the lower right quadrant of her visual field (Fig. 3(b)). We also tested a normal control subject, MH, aged 32 years, with normal uncorrected visual acuity and visual fields. We used the retinotopic mapping paradigm detailed in the section describing the cortical representation of the visual field in achromats. For this study, however, the visual stimulus extended to 5° of visual angle, because we were principally concerned with evaluating central visual function. Seven complete cycles of the quadrant and annular stimuli were presented during acquisition of T2* MR images. The functional MR images were acquired using a Siemens Magnetom Vision 1.5 T MRI system fitted with EPI gradient overdrive. Sequence and imaging

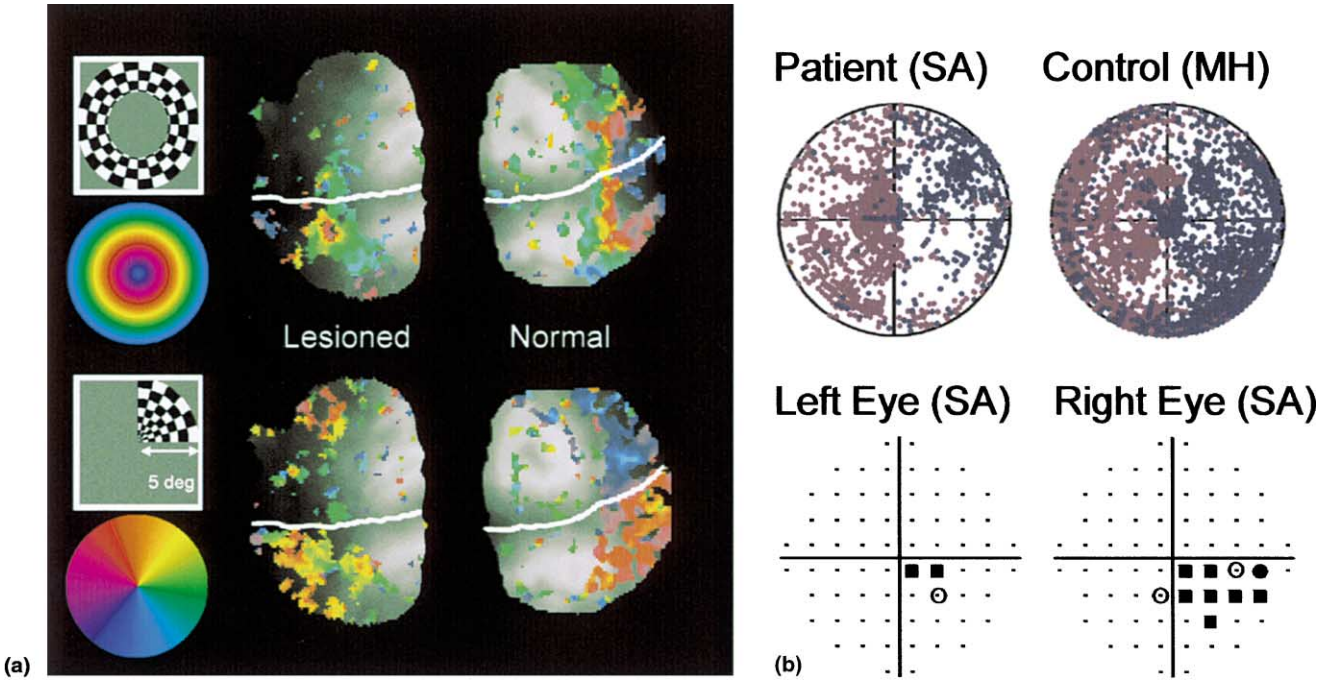

Fig. 3. (a) Flattened representations of the left (to the left) and right (to the right) hemispheres of subject SA. Superimposed on the flattened grey matter are false colour maps that indicate the representations of eccentricity (top) and polar angle (bottom) following the colour keys shown to the left of the figure. All signals exceed a correlation of 0.25. Inset to the left are schematic representations of the stimuli presented to the subject. (b) Plots of the visual field co-ordinates to which voxels responded. Co-ordinates for voxels originating from the left and right hemispheres are shown in blue and purple, respectively. Data for the patient SA and control MH are to the left and right, respectively, and each plot is for a visual field of $\pm 5°$. On the bottom row of the figure visual field plots obtained from Humphrey perimetry that survey $\pm 10°$ for the left and the right eye.

parameters were identical to those described for imaging the albino subject. For rotating quadrants images were acquired perpendicular to the calcarine sulcus whereas for stimulation with annuli the images were acquired parallel to the calcarine sulcus. The MPRAGE imaging sequence was used to acquire anatomical T1-weighted images ($0.98 \times 0.98 \times 1$ mm^3) on the same scanner.

We present the cortical activations on flattened representations of the occipital lobe in Fig. 3(a). Voxels exceeding a correlation of 0.2 are displayed after smoothing with a Gaussian kernel (S.D. 1.4 mm, width 5 mm). The patient's right hemisphere displays a normal pattern of activation for stimulation with expanding rings and rotating wedges. The expanding rings elicited a smooth progression in the phase of the activation from the occipital pole to anterior cortex, indicating the representation of eccentricity in the occipital lobe. The rotating wedges elicited activity in much the same regions of cortex, which is consistent as identical regions of the visual field are stimulated in each experiment. For the rotating wedges the phase progression is approximately perpendicular to that observed in response to expanding rings. The vertical meridians, indicated by cyan and orange, delimit the visual area boundaries. V1 can be clearly identified, but extrastriate areas are not easily seen in this data set. The lesioned hemisphere displays an abnormal pattern of activations in response to expanding rings and rotating wedges. The smooth progression of phase of activations in response to rings is only observed in ventral regions of the occipital lobe. Some activity is observed dorsal to the calcarine sulcus, but only at phases that indicate responsivity beyond 3°. Stimulation with rotating wedges elicited a patchy response from the patients occipital lobe. The most extensive region of activation was sub-calcarine and was similarly located to activations observed in response to expanding rings. There was additional activation superior to the calcarine sulcus, but in common with all activations the response phase indicated a selectivity to the upper visual field. Responses in dorsal cortex to superior visual field locations are not unexpected on the basis of hemifield representations that have been documented previously.

Qualitatively, therefore, the retinotopic mapping experiments have revealed an absence of sensitivity to the lower right quadrant within 3° of fixation. In order to visualize this lack of sensitivity, we have constructed a visual field plot from the fMRI data sets presented in Fig. 3(b). We determined the polar angle and eccentricity co-ordinates of voxels by combining the phase information derived from the two experiments we conducted. We then plot the co-ordinates of each voxel in polar form such that it resembles a visual field plot obtained with perimetry. The visual field representation for the patient and a normal control are illustrated in the upper row of Fig. 3(b). The visual field co-ordinates of voxels from the patient's and control's right hemispheres are found to principally be in the left hemifield. The distribution of co-ordinates is reasonably even. The voxels originating from the left hemisphere in the control have visual field co-ordinates that are principally distributed in the right hemifield. In contrast, voxels measured in the patient's left hemisphere only appear to represent strongly the upper right region of the visual field. There is very sparse representation of the inferior right visual field in the patient. We obtained a visual field plot with Humphrey perimetry (lower row of

Fig. 3(b)). The field plots also indicate a lack of sensitivity to the lower right regions of the visual field, with stimuli presented at x, y co-ordinates of 1°, −1° and 3°, −1° eliciting no response from the patient in both eyes. There is good agreement, therefore, between the visual field co-ordinates for which no fMRI or behavioural response could be measured.

This study highlights the potential of fMRI to aid the interpretation of visual deficits that result from lesion. The patient we describe here had no lesion to early visual areas in contrast to a well studied patient, GY, who we have also studied (Baseler et al., 1999). There was a lesion to white matter, most probably the optic radiation, which could have compromised the input to V1. We were able to show directly that there was no measurable activity in intact grey matter that normally would have been responsive to visual field locations that represented the lower right visual field near fixation. We can be confident, therefore, that the behavioural visual loss is a result of a lack on innervation of V1. Without fMRI measurements this conclusion would have to remain an inference.

4. Conclusions

In this article we have concentrated on the way in which the visual field is mapped onto the cortical surface. We have examined visual abnormalities that give rise to abnormal cortical representations. The visual abnormalities are results of lesion to different levels of the visual system. In rod achromats the central retina is not light sensitive, but we were able to show that the cortex that normally receives input from that region is driven by light generated signals in rods. This leads to an abnormal cortical representation in the respect that the cortical magnification factor is significantly altered from normal. Our interpretation of this change is based on a reorganisation of the cortex following visual experience. The albino visual system is abnormally wired with a larger number of retinal afferents crossing at the optic chiasm. We were able to show that the abnormally crossed fibres stimulated cortex, which is inconsistent with some suggestions of suppression of these signals (Guillery, 1986). We were also able to show that the signals originating from mirror symmetrical positions in opposing hemifields projected to common cortical sites. This finding is not consistent with the Boston projection pattern in albinism (Hubel & Wiesel, 1971). Further experimentation on albino subjects will be able to reveal if there is variation in the manner in which the visual field is represented in hypopigmented humans. Finally, we were able to assess the impact of a cortical lesion on the activity in the visual cortex. The lesion did not affect the cortical grey matter that is usually activated by central visual field. However, the lack of activity that we documented in response to stimulation of the central lower right visual field indicated that the lesion was most likely affecting the optic radiation and hence input to V1.

The cases we have presented are attempts to evaluate the manner in which the visual cortex deals with abnormal input, be it a result of a retinal, chiasmatic of cortical abnormality. In the two former developmental disorders the cortex appears to have very different visual representations, that at least in rod achromats represents

reorganization. In the case of lesion, the acquired nature of the damage led to a loss of activity in calcarine cortex and no measurable reorganization. Overall, we hope to have shown the value of measuring cortical responses in patients with abnormal visual function, firstly to address neuroscientific issues associated with how the brain may deal with abnormal input, and secondly to put forward the retinotopic mapping technique as useful in determining the underlying cause of visual dysfunction in cases of acquired lesions. The studies presented here also prompt further investigations into what visual benefit may be derived from an enlarged cortical representation of peripheral visual signals in rod achromats and what behavioural problems that may result from mirror symmetric positions in the visual field occupying neighbouring points in albino cortex.

Acknowledgements

ABM and MH acknowledge with thanks the Wellcome Trust for grant support.

References

Apkarian, P. (1992). A practical approach to albino diagnosis. VEP misrouting across the age span. *Ophthalmic Paediatric Genetics*, *13*, 77–88.

Barbur, J. L., Watson, J. D., Frackowiak, R. S., & Zeki, S. (1993). Conscious visual perception without V1. *Brain*, *116*, 1293–1302.

Barton, J. J., Simpson, T., Kiriakopoulos, E., Stewart, C., Crawley, A., & Guthrie, B., et al. (1996). Functional MRI of lateral occipitotemporal cortex during pursuit and motion perception. *Annals of Neurology*, *40*, 387–398.

Baseler, H. A., Morland, A. B., & Wandell, B. A. (1999). Topographic organization of human visual areas in the absence of input from primary cortex. *Journal of Neuroscience*, *19*, 2619–2627.

Boynton, G. M., Engel, S. A., Glover, G. H., & Heeger, D. J. (1996). Linear systems analysis of functional magnetic resonance imaging in human V1. *Journal of Neuroscience*, *16*, 4207–4221.

Clarke, S., & Miklossy, J. (1990). Occipital cortex in man: organization of callosal connections, related myelo- and cytoarchitecture, and putative boundaries of functional visual areas. *Journal of Computational Neurology*, *298*, 188–214.

Clarke, S., Walsh, V., Schoppig, A., Assal, G., & Cowey, A. (1998). Colour constancy impairments in patients with lesions of the prestriate cortex. *Experimental Brain Research*, *123*, 154–158.

Creel, D. J. (1971). Visual system anomaly associated with albinism in the cat. *Nature*, *231*, 465–466.

Dale, A. M., Fischl, B., & Sereno, M. I. (1999). Cortical surface-based analysis. I. Segmentation and surface reconstruction. *NeuroImage*, *9*, 179–194.

Damasio, A., Yamada, T., Damasio, H., Corbett, J., & McKee, J. (1980). Central achromatopsia: behavioral, anatomic, and physiologic aspects. *Neurology*, *30*, 1064–1071.

DeYoe, E. A., Bandettini, P., Neitz, J., Miller, D., & Winans, P. (1994). Functional magnetic resonance imaging (fMRI) of the human brain. *Journal of Neuroscience Methods*, *54*, 171–187.

DeYoe, E. A., Carman, G. J., Bandettini, P., Glickman, S., Wieser, J., & Cox, R., et al. (1996). Mapping striate and extrastriate visual areas in human cerebral cortex. *Proceedings of the National Academy of Sciences USA*, *93*, 2382–2386.

Drury, H. A., Van Essen, D. C., Anderson, C. H., Lee, C. W., Coogan, T. A., & Lewis, J. W. (1996). Computerized mappings of the cerebral cortex: a multiresolution flattening method and a surface-based coordinate system. *Journal of Cognitive Neuroscience*, *8*, 1–28.

Engel, S. A., Glover, G. H., & Wandell, B. A. (1997). Retinotopic organization in human visual cortex and the spatial precision of functional MRI. *Cerebral Cortex*, *7*, 181–192.

Engel, S. A., Rumelhart, D. E., Wandell, B. A., Lee, A. T., Glover, G. H., & Chichilnisky, E. J., et al. (1994). fMRI of human visual cortex [letter]. *Nature*, *369*, 525.

Estevez, O., & Spekreijse, H. (1982). The "silent" substitution method in visual research. *Vision Research*, *22*, 681–691.

Fischl, B., Sereno, M. I., & Dale, A. M. (1999). Cortical surface-based analysis II: Inflation, flattening, and a surface-based coordinate system. *NeuroImage*, *9*, 195–207.

Guillery, R. W. (1969). An abnormal retinogeniculate projection in Siamese cats. *Brain Research*, *14*, 739–741.

Guillery, R. W. (1971). An abnormal retinogeniculate projection in the albino ferret (Mustela furo). *Brain Research*, *33*, 482–485.

Guillery, R. W. (1974). Visual pathways in albinos. *Scientific American*, *230*, 44–54.

Guillery, R. W. (1986). Neural abnormalities of albinos. *Trends in Neurosciences*, *18*, 364–367.

Guillery, R. W., Hickey, T. L., Kaas, J. H., Felleman, D. J., Debruyn, E. J., & Sparks, D. L. (1984). Abnormal central visual pathways in the brain of an albino green monkey (Cercopithecus aethiops). *Journal Comparative Neurology*, *226*, 165–183.

Guillery, R. W., Okoro, A. N., & Witkop, C. J. (1975). Abnormal visual pathways in the brain of a human albino. *Brain Research*, *96*, 373–377.

Hedera, P., Lai, S., Haacke, E. M., Lerner, A. J., Hopkins, A. L., & Lewin, J. S., et al. (1994). Abnormal connectivity of the visual pathways in human albinos demonstrated by susceptibility-sensitized MRI [see comments]. *Neurology*, *44*, 1921–1926.

Heinen, S. J., & Skavenski, A. A. (1991). Recovery of visual responses in foveal V1 neurons following bilateral foveal lesions in adult monkey. *Experimental Brain Research*, *83*, 670–674.

Hess, R. F., Mullen, K. T., Sharpe, L. T., & Zrenner, E. (1989). The photoreceptors in atypical achromatopsia. *Journal of Physiology (London)*, *417*, 123–149.

Holmes, G. (1918). Disturbances of vision caused by cerebral lesions. *British Journal of Ophthalmology*, *2*, 353–384.

Horton, J. C., & Hoyt, W. F. (1991a). The representation of the visual field in human striate cortex. A revision of the classic Holmes map. *Archives of Ophthalmology*, *109*, 816–824.

Horton, J. C., & Hoyt, W. F. (1991b). Quadrantic visual field defects. A hallmark of lesions in extrastriate (V2/V3) cortex. *Brain*, *114*, 1703–1718.

Hubel, D. H., & Wiesel, T. N. (1971). Aberrant visual projections in the Siamese cat. *Journal of Physiology (London)*, *218*, 33–62.

Hubel, D. H., & Wiesel, T. N. (1974). Uniformity of monkey striate cortex: a parallel relationship between field size, scatter, and magnification factor. *Journal Comparative Neurology*, *158*, 295–305.

Kaas, J. H., & Guillery, R. W. (1973). The transfer of abnormal visual field representations from the dorsal lateral geniculate nucleus to the visual cortex in Siamese cats. *Brain Research*, *59*, 61–95.

Kennard, C., Lawden, M., Morland, A. B., & Ruddock, K. H. (1995). Colour identification and colour constancy are impaired in a patient with incomplete achromatopsia associated with prestriate cortical lesions. *Proceedings of the Royal Society, London B Biological Sciences*, *260*, 169–175.

Kohl, S., Baumann, B., Broghammer, M., Jagle, H., Sieving, P., & Kellner, U., et al. (2000). Mutations in the CNGB3 gene encoding the beta-subunit of the cone photoreceptor cGMP-gated channel are responsible for achromatopsia (ACHM3) linked to chromosome 8q21. *Human Molecular Genetics*, *9*, 2107–2116.

Kohl, S., Marx, T., Giddings, I., Jagle, H., Jacobson, S. G., & Apfelstedt-Sylla, E., et al. (1998). Total colourblindness is caused by mutations in the gene encoding the alpha-subunit of the cone photoreceptor cGMP-gated cation channel. *Nature Genetics*, *19*, 257–259.

Lund, R. D. (1965). Uncrossed visual pathways of hooded and albino rats. *Science*, *149*, 1506–1507.

Sahraie, A., Weiskrantz, L., Simmons, A., Williams, S. C. R., & Barbur, J. L. (1996). Conscious and unconscious processing of visual signals: psychophysical and fMRI studies. *Perception*, *25*, 1372–1372.

Sereno, M. I., Dale, A. M., Reppas, J. B., Kwong, K. K., Belliveau, J. W., & Brady, T. J., et al. (1995). Borders of multiple visual areas in humans revealed by functional magnetic resonance imaging [see comments]. *Science*, *268*, 889–893.

Sharpe, J. A., & Wong, A. M. F. (1997). Representation of the visual-field in human occipital cortex: a correlation between magnetic resonance imaging and visual-field defects. *Investigative Ophthalmology & Visual Science*, *38*, 2906–2906.

Sharpe, L. T., Fach, C., & Nordby, K. (1988). Temporal summation in the achromat. *Vision Research*, *28*, 1263–1269.

Teo, P. C., Sapiro, G., & Wandell, B. A. (1997). Creating connected representations of cortical gray matter for functional MRI visualization. *IEEE Transactions in Medical Imaging*, *16*, 852–863.

Tootell, R. B., Dale, A. M., Sereno, M. I., & Malach, R. (1996). New images from human visual cortex. *Trends in Neuroscience*, *19*, 481–489.

Tootell, R. B. H., Switkes, E., Silverman, M. S., & Hamilton, S. L. (1988). Functional anatomy of macaque striate cortex. 2. Retinotopic organization. *Journal of Neuroscience*, *8*, 1531–1568.

Zeki, S., & Ffytche, D. H. (1998). The Riddoch syndrome: insights into the neurobiology of conscious vision. *Brain*, *121*, 25–45.

Zeki, S., Watson, J. D., Lueck, C. J., Friston, K. J., Kennard, C., & Frackowiak, R. S. (1991). A direct demonstration of functional specialization in human visual cortex. *Journal of Neuroscience*, *11*, 641–649.

Zeki, S. M. (1977). Simultaneous anatomical demonstration of the representation of the vertical and horizontal meridians in areas V2 and V3 of rhesus monkey visual cortex. *Proceedings of the Royal Society, London B Biological Sciences*, *195*, 517–523.

Zihl, J., von Cramon, D., & Mai, N. (1983). Selective disturbance of movement vision after bilateral brain damage. *Brain*, *106*, 313–340.